PHYSICAL REVIEW A VOLUME 60, NUMBER 6 DECEMBER 1999

Electron capture and excitation in collisions of Si^{2+} ions with He atoms at intermediate energies

S. Suzuki and N. Shimakura
Faculty of Science, Niigata University, Niigata 950-21, Japan

J.-P. Gu,* G. Hirsch, and R. J. Buenker*
Theoretische Chemie, Bergische Universität-Gesamthochschule Wuppertal, D-42097 Wuppertal, Germany

M. Kimura
School of Medicine, Yamaguchi University, Ube, 755 Yamaguchi, Japan

P. C. Stancil
Physics Division, Oak Ridge National Laboratory, Oak Ridge, Tennessee 37831

(Received 23 November 1998)

We have investigated electron capture and excitation in collisions of Si^{2+} ions with He atoms in the collision energy range from 0.02–6 keV/u based on a molecular representation. Molecular states are determined by using the multireference single- and double-excitation configuration-interaction method. We have considered electron capture and excitation both by the ground singlet and metastable triplet Si^{2+} ions. The capture cross section by the ground singlet Si^{2+} ion increases with increasing collision energy and reaches a value of $\sim 1.5\times 10^{-16}\,cm^2$, while that by the metastable triplet ion is found to be large with a magnitude of $4\times 10^{-16}\,cm^2$ at the highest energy studied. Weak but conspicuous oscillatory structures are found for both cases, which are due to multichannel interference. The present rate coefficient for the ground singlet Si^{2+} ion impact is found to be much smaller than those of the $[Si^{4+}+He]$ system studied earlier.
[S1050-2947(99)01311-6]

PACS number(s): 34.50.−s, 34.20.Mq, 34.70.+e

I. INTRODUCTION

Reaction processes which involve Si^{q+} ions in collisions with H, H_2, He, and other neutral species have recently attracted a great deal of interest due to their potential application in astrophysics, fusion research, and thin microfilm technology [1]. However, the majority of studies have been concerned with H atomic targets [2–5], and to the best of our knowledge, there are only six theoretical investigations for He targets [6–11]. Butler and Dalgarno [6] estimated the rate constants for the electron-capture process in ion-atom collisions, i.e., $[Si^{3+}, Si^{4+}+He]$, and the reverse processes, $[Si^{+}, Si^{2+}+He^{+}]$, by using a simple Landau-Zener method for a few temperatures between 1000 and 31 600 K. Opradolce, McCarroll, and Valiron [7] and Stancil *et al.* [8] have also treated the electron-capture process in $[Si^{4+}+He]$ collisions at low energies, 1 meV/u–1 keV/u and 3 meV/u–10 eV/u, respectively, both based on the molecular representation. Stancil *et al.* [8] have noted that these two theoretical results are in qualitative agreement but that there are some unresolved discrepancies at the low and high ends of the energy region they studied. Recently, Bacchus-Montabonel and Ceyzeriat [11] reported electron-capture cross sections for $[Si^{4+}+He]$ collisions. At the lower-energy end of their calculation, fair agreement with the results of Stancil *et al.* [8] was found. Further, the only experimental data [12] are in significant disagreement with all available theoretical results. The $[Si^{3+}+He]$ system has only been studied recently in the molecular representation [9,10]. Both results are in fair agreement with the experimental data of Fang and Kwong [13].

However, until now there has been no theoretical or experimental study of the $[Si^{2+}+He]$ system, which may also be important for astrophysical environments as well as Si thin-film manufacturing with ion-beam technology. In x-ray dissociation regions of interstellar clouds, multiply charged ions can coexist with H_2 and He, with atomic H usually being of small abundance. Fast sequential charge transfer reduces the multiply charged ions to singly charged, but for the case of many doubly charged ions charge transfer may be slow or have a significant energy threshold, therefore creating a bottleneck in this charge-transfer cascade and a significant population of doubly charged ions. Si^{2+} is just such a case as it is expected to have small charge-transfer rate coefficients for collisions with H_2 and He. It is then important to obtain accurate rate coefficients to be able to predict the abundance of Si^{2+} and its expected emission flux. In technological applications, Si-ion beams are expected to play a major role for future ion-beam-based thin-film manufacturing. These ions are charge transferred, hence becoming neutral Si atoms before they reach surfaces for deposition. As described above, a precise knowledge of charge transfer rates for collisions with H_2 and other molecules are essential for successful production of thin films. Therefore, we conduct a theoretical investigation of electron capture resulting from $Si^{2+}+He$ collisions within the molecular representation be-

---

*Present address: Institute for Theoretical Atomic and Molecular Physics, Harvard-Smithsonian Center for Astrophysics, 60 Garden St. Cambridge, MA 02138.

low 6 keV/u. The processes we are concerned with are (i) the projectile ground state:

$$\mathrm{Si}^{2+}(^1S)+\mathrm{He}\rightarrow\mathrm{Si}^{+}(^2P^o)+\mathrm{He}^{+}\quad\text{electron capture,}\tag{1a}$$

$$\rightarrow\mathrm{Si}^{2+}(^1P^o)+\mathrm{He}\quad\text{projectile excitation,}\tag{1b}$$

(ii) the projectile metastable state:

$$\mathrm{Si}^{2+}(^3P^o)+\mathrm{He}\rightarrow\mathrm{Si}^{+}(^2P^o)+\mathrm{He}^{+}\quad\text{electron capture,}\tag{2a}$$

$$\rightarrow\mathrm{Si}^{+}(^4P)+\mathrm{He}^{+}\quad\text{electron capture.}\tag{2b}$$

The triplet state lies above the ground singlet state by 6.52 eV. All processes, both in the singlet and triplet manifolds, are endoergic with a larger energy defect between the initial and capture channels in the singlet manifold. Therefore, the contribution from the triplet is expected to be dominant for scattering dynamics. However, it is important to verify this quantitatively.

II. SUMMARY OF THE THEORETICAL METHODS AND CALCULATIONS

Details of the theoretical treatment in this paper have been already described earlier [14–17], and hence only the specific information used in the present paper is shown.

A. Molecular states

The AO basis set used in the calculation for the silicon atom is the $(13s10p4d1f)$ basis contracted to $[10s7p4d1f]$ [18], but a new exponent of 0.34 for the f function is obtained from reoptimization and used in the present calculation. It is found that the calculated excitation energies of the low-lying states for both Si^+ and Si^{2+} ions agree with experimental values quite satisfactorily when using the present basis set. For helium, the s- and p-type functions are from Ref. [19]. Additionally, three d-type functions [20] are added and the final contracted basis set is $(10s5p3d)/[7s4p3d]$.

The potentials and coupling matrix elements are computed using the multireference single- and double-excitation configuration-interaction (MRD-CI) method [21], with configuration selection and energy extrapolation employing the table CI algorithm [22] for the range of Si–He internuclear distances from 2.0 to $20.0a_0$. In the CI calculations, the five lowest molecular orbitals are always kept doubly occupied, whereas the five highest ones are discarded. A small selection threshold [21] of $2\times10^{-7}E_h$ (in units of Hartrees) has been used in the present treatment. More details of the present MRD-CI calculations can be found in Table I. The radial coupling matrix elements are obtained using calculated MRD-CI wave functions in a finite-difference method [23].

B. Collision dynamics

A semiclassical molecular-state expansion method has been employed at collision energies from 20 eV/u to 6 keV/u. A total scattering wave function is expanded in terms of the product of an electronic wave function and an electron-translation factor. Substituting the total wave function into the time-dependent Schrödinger equation yields a set of coupled equations, which are solved numerically under the assumption of straightline trajectories for heavy-particle motion. By squaring the resulting amplitude, the transition probability is obtained as a function of collision energy and impact parameter. The cross section is given by an integration of impact-parameter-weighted transition probability over the impact parameter. States included are (i) for the singlet manifold, the initial 1 $^1\Sigma^+$ channel, electron capture 2 $^1\Sigma^+$, 1 $^1\Pi$ channels, and excitation 3 $^1\Sigma^+$, 2 $^1\Pi$ channels and (ii) for the triplet manifold, the initial 1 $^3\Sigma^+$, 1 $^3\Pi$ channels, electron capture 2 $^3\Sigma^+$, 2 $^3\Pi$, 1 $^3\Sigma^-$, and 3 $^3\Pi$ channels as described in more detail below.

TABLE I. Number of reference configurations, N_{ref}, and number of roots, N_{root}, treated in each irreducible representation and the corresponding number of generated (N_{tot}) and selected (N_{sel}) symmetry-adapted functions for a threshold of $0.2\times10^{-6}E_h$ at an Si-He internuclear distance of $2.6a_0$.

State	$N_{\mathrm{ref}}/N_{\mathrm{root}}$	N_{tot}	N_{sel}
$^1A_1$	118/7	214 225	25 070
$^1B_1$	72/4	158 300	17 718
$^1A_2$	56/2	145 407	10 280
$^3A_1$	104/5	305 449	32 143
$^3B_1$	84/5	259 980	29 779
$^3A_2$	59/3	231 034	22 246

III. RESULTS AND DISCUSSIONS

A. Adiabatic potentials and dynamical couplings

All the states from the singlet and triplet manifolds used in the calculation are listed in Table II with corresponding asymptotic atomic levels. Two quintet states, 1 $^5\Sigma^-$ and 1 $^5\Pi$, which correspond to the $\mathrm{Si}^+(^4P)/\mathrm{He}^+(^2S)$ channel are not calculated since the effect of spin-orbit interaction in the collision process is expected to be negligible. The $\mathrm{Si}^+(^2D)+\mathrm{He}^+(^2S)$ channel, which lies 12 480 cm^{-1} above the $\mathrm{Si}^+(^4P)+\mathrm{He}^+(^2S)$ channel, corresponds to three singlet and three triplet states. These states are not included in the collision calculation.

It can be seen that the present calculated asymptotic relative energies (at $R=50.0a_0$) for all the states agree well with those derived from available experimental data [24]. Note that for the states corresponding to the $\mathrm{Si}^+/\mathrm{He}^+$ channels, an energy value of $0.02E_h$ is already subtracted in Table II to account for the Coulomb repulsion of the positive ions at $R=50a_0$.

The potential curves for SiHe^{2+} are shown in Figs. 1(a) and 1(b) for the singlets and triplets, respectively. It should be noted that for the singlet manifold near $R=13.5a_0$, there are two avoided crossings between the 1 $^1\Pi$ and 2 $^1\Pi$ states as well as the 2 $^1\Sigma^+$ and 3 $^1\Sigma^+$ states. Accordingly, the slopes of these states change abruptly there. At around $4a_0$, a few strongly avoided crossings are present among higher-lying states including 3 $^1\Sigma^+$ and 2 $^1\Pi$ states, which are expected to play an important role for exit of the flux to higher levels through a ladder-climbing mechanism at higher-collision energies.

TABLE II. Calculated relative energies of the electronic states of SiHe^{2+} at the asymptotic limit ($R=50.0a_0$).

Asymptote	States	Calculated energy (E_h)[a]	Relative energy (cm^{-1})[b]	Experimental (cm^{-1})
$\mathrm{Si}^{2+}(^1S)/\mathrm{He}(^1S)$	$1\ ^1\Sigma^+$	−290.938 65	0	0
$\mathrm{Si}^{2+}(^3P^o)/\mathrm{He}(^1S)$	$1\ ^3\Sigma^+$	−290.704 32	51 429	52 984
	$1\ ^3\Pi$	−290.704 31	51 432	
$\mathrm{Si}^{+}(^2P^o)/\mathrm{He}^{+}(^2S)$	$2\ ^1\Sigma^+$	−290.614 71	66 707	66 664
	$1\ ^1\Pi$	−290.614 37	66 782	
	$2\ ^3\Sigma^+$	−290.614 68	66 714	
	$2\ ^3\Pi$	−290.614 33	66 790	
$\mathrm{Si}^{2+}(^1P^o)/\mathrm{He}(^1S)$	$3\ ^1\Sigma^+$	−290.561 67	82 737	82 884
	$2\ ^1\Pi$	−290.561 70	82 731	
$\mathrm{Si}^{+}(^4P^o)/\mathrm{He}^{+}(^2S)$	$1\ ^3\Sigma^-$	−290.426 88	107 931	109 666
	$3\ ^3\Pi$	−290.426 27	108 065	

[a] Original calculated values for all states.

[b] Corrected values by subtracting $0.02E_h$ for those states corresponding to $\mathrm{Si}^+/\mathrm{He}^+$ channels (see text).

For the triplet manifold, the initial $1\ ^3\Sigma^+$ and $1\ ^3\Pi$ states show no obvious avoided crossing within the present R region since all excited states are well separated energetically. Electron-capture states $[2\ ^3\Sigma^+$ and $2\ ^3\Pi]$ are located nearest to the initial state with the asymptotic energy separation of 1.7 eV. In the region of $R=3-4a_0$, similar to the singlet manifold, there are a few avoided crossings among the excited states. However, because of the lack of an avoided crossing with the initial state, the corresponding dynamical coupling should be relatively weak. Nonetheless, they are energetically more dense than their counterparts of the singlet manifold, hence suggesting a stronger transition probability than that for the singlet manifold.

The potential of the ground $1\ ^1\Sigma^+$ state of the SiHe^{2+}, which asymptotically corresponds to the $[\mathrm{Si}^{2+}(^1S)+\mathrm{He}]$ channel, is very flat in the region near the energy minimum, and in such a case it is quite difficult to determine an accurate equilibrium distance, R_e, value. According to the present calculations, the $1\ ^1\Sigma^+$ state has a shallow potential minimum located at $R_e=4.39a_0$, which is smaller than previously reported theoretical values [25–27]. In Table III, R_e values, which give the potential minimum for some selected states and adiabatic energy differences ΔE, are presented, together with those available in the literature. Note that the potentials of the $2\ ^1\Sigma^+$, $1\ ^1\Pi$, and $1\ ^3\Sigma^-$ become dissociative at infinity.

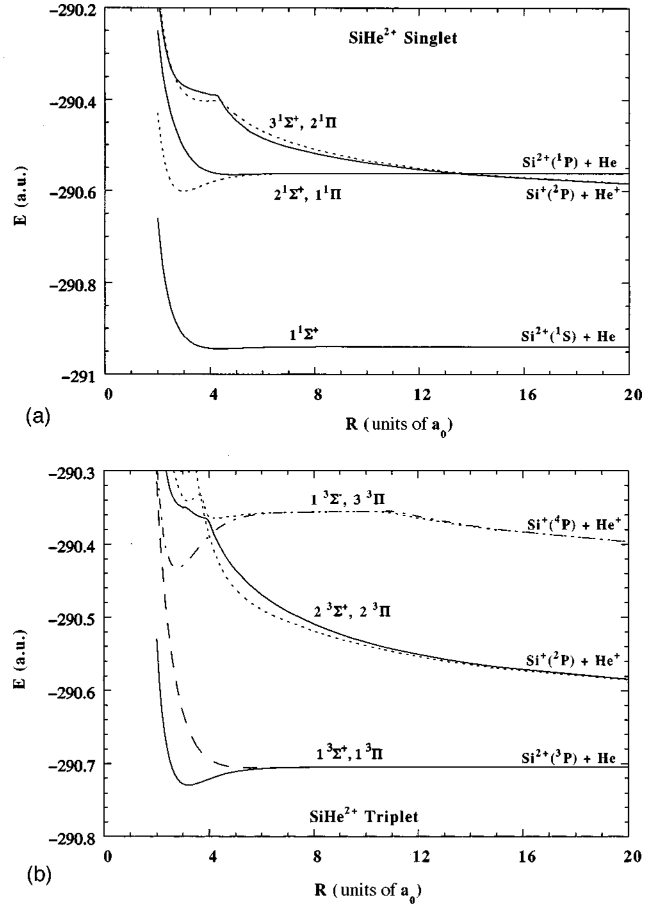

FIG. 1. (a) Adiabatic potentials of the singlet $(\mathrm{SiHe})^{2+}$ system. (b) Adiabatic potentials of the triplet $(\mathrm{SiHe})^{2+}$ system.

TABLE III. Potential minima, R_e, and adiabatic energy differences, ΔE, between the selected excited states and the ground state of SiHe^{2+}, and comparison with earlier theoretical results.

State	$R_e(a_0)$	ΔE (eV)
$1\ ^1\Sigma^+$	4.39	0.0
	4.853[a]	
	5.244[b]	
	5.422[c]	
$1\ ^3\Pi$	3.22	5.84
	3.211[a]	
	3.290[b]	
$1\ ^1\Pi$	3.00	9.31
$2\ ^1\Sigma^+$	4.87	10.3
$1\ ^3\Sigma^-$	2.78	13.9
	2.819[b]	

[a] Reference [25].

[b] Reference [26].

[c] Reference [27].

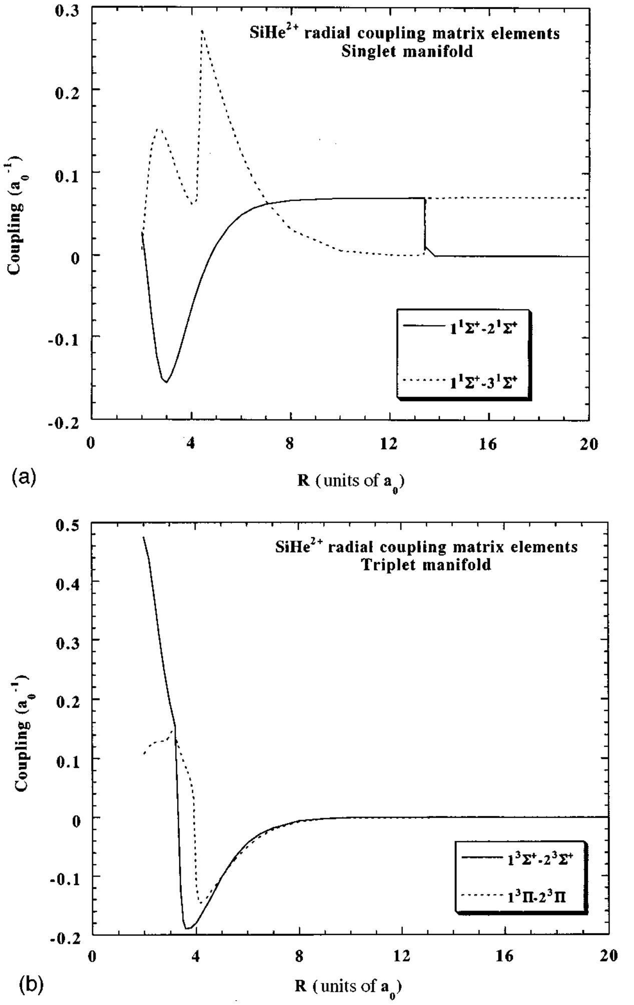

FIG. 2. (a) Representative nonadiabatic coupling matrix elements for the singlet manifold. (b) Representative nonadiabatic coupling matrix elements for the triplet manifold.

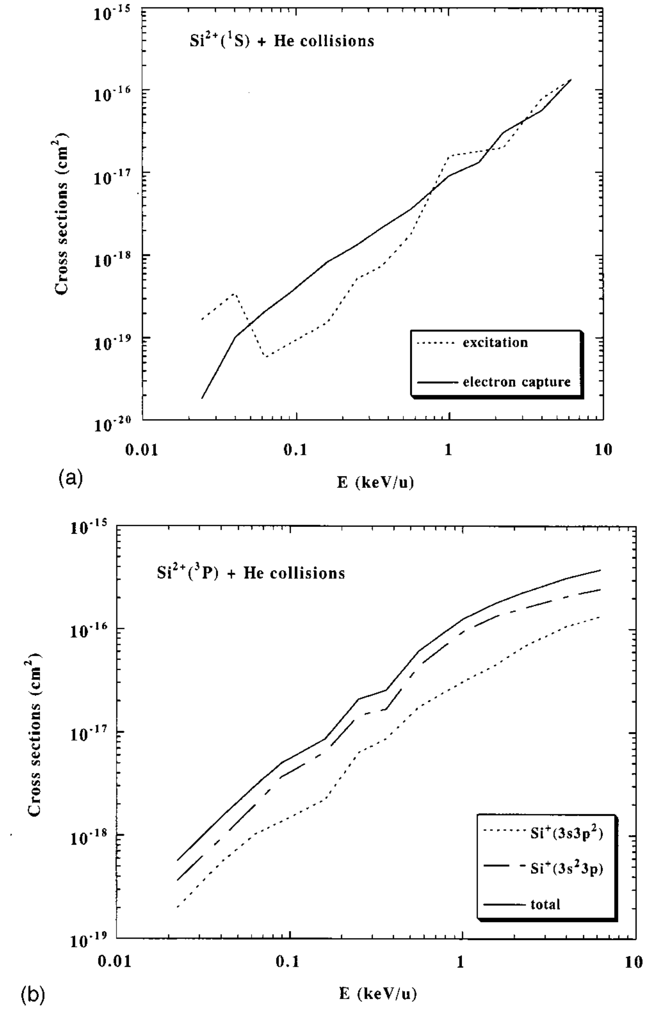

FIG. 3. (a) Cross sections for electron capture and excitation in collisions of the ground Si^{2+} (^1S) ions with He atom. The solid line is for electron capture and the dotted line is for excitation. (b) Cross sections for electron capture in collisions of the excited Si^{2+} ($^3P^o$) ions with He atom. The dotted line is for Si$^+$($3s3p^2$) formation, the dash-dotted line is for Si$^+$($3s^23p$) formation, and the solid line is for the sum of both.

Representative radial coupling and rotational coupling elements are shown in Figs. 2(a) and 2(b). These matrix elements reflect some prominent features in the adiabatic potentials discussed above.

B. Cross sections

In the present collision system, the Si^{2+} ion and the He atom are considered to be mostly in the ground electronic state under usual conditions. In such a case, the initial channel corresponds to the singlet $1\ ^1\Sigma^+$ molecular state, i.e., [Si^{2+}($3s^2$; ^1S)+He($1s^2$; ^1S)]. However, the lowest excited state of the Si^{2+} ion ($3s^13p^1$; $^3P^o$) is located at about 6.5 eV above the ground Si^{2+} ion state, so electron capture by the lowest excited Si^{2+} ion is also interesting.

For the reaction from the electronic ground state [Si^{2+}(^1S)+He(^1S)], the five molecular states shown in Fig. 1(a), which correspond to electron capture [$2\ ^1\Sigma^+$, $1\ ^1\Pi$; Si$^+$($3s^23p^1$; $^2P^o$)+He$^+$($1s^1$; ^2S)] and excitation [$3\ ^1\Sigma^+$, $2\ ^1\Pi$; Si^{2+}($3s^13p^1$; $^1P^o$)+He($1s^2$; ^1S)], were included in the dynamical calculations. Corresponding energy splittings between $2\ ^1\Sigma^+$ and $3\ ^1\Sigma^+$, and $1\ ^1\Pi$ and $2\ ^1\Pi$ at the crossings around $R=13.5a_0$ are quite small with values less than 10^{-4} a.u. and the preliminary calculations show that the flux passes through these avoided crossings with a probability greater than 99.9%. Therefore, in what follows, we treat the crossings diabatically.

For the processes from the metastable triplet state [Si^{2+}($3s^13p^1$; ^3P)+He(^1S)], the six molecular states displayed in Fig. 1(b) that correspond to electron capture [Si$^+$($3s^23p^1$; $^2P^o$)+He$^+$($1s^1$; ^2S); $2\ ^3\Sigma^+$, $2\ ^3\Pi$], and [Si$^+$($3s^13p^2$; ^4P)+He$^+$($1s$; ^2S); $1\ ^3\Sigma^-$, $3\ ^3\Pi$] states, in addition to the initial $1\ ^3\Sigma^+$ and $1\ ^3\Pi$ states, were included in the scattering calculations. In this case, $1\ ^3\Sigma^+$ and $1\ ^3\Pi$ states can be considered as the initial state, so we have determined the cross sections by multiplying each state by its statistical weight. It should be noted that the spin-orbit interaction is not important in the collision energies considered, so it was neglected.

1. Electron capture and excitation by ground Si^{2+}(^1S) ion impact

Figure 3(a) shows our calculated cross sections for the electron capture and excitation processes by the ground

$Si^{2+}(3s^2{:}\,^1S)$ ion impact. The total cross sections [the sum of capture $Si^{+}(3s^23p)$ and excitation to $Si^{2+}(3s3p)$] are rather small, in particular at low collision energies, and they increase with increasing collision energy. This is a typical characteristic for an endoergic system, in which there is no strong avoided crossing between the initial, and electron capture and excitation channels. As shown in Fig. 1(a), the potential-energy difference between the initial, and electron capture and excitation channels is quite large except at small internuclear distances, so the electron-capture and excitation processes should occur at relatively small internuclear distances ($R < 2.5a_0$) and at relatively large collision energies for ions to penetrate deep inside the target. At lower collision energies, the electron-capture process of the $Si^{+}(3s^23p^1{:}\,^2P^o)$ state becomes dominant over the excitation process to the $Si^{2+}(3s^13p^1{:}\,^1P^o)$ state except for the two lowest energies. However, at higher collision energies, both processes have similar cross section magnitude, suggesting a strong mixing of the flux among these channels. The two cross sections oscillate in an out-of-phase manner above 1 keV/u, but the oscillations are more frequent and conspicuous in the excitation cross section over the entire energy range because these levels are somewhat weaker channels. Such oscillations are a common prediction of modern molecular-orbital calculations and are usually attributed to phase interferences between different reaction pathways in a multichannel scattering problem. For an alternative viewpoint, see Ref. [28]. The transition to the $3\,^1\Sigma^+$ and $2\,^1\Pi$ states occurs by a two-step mechanism, i.e., first the transition to the $2\,^1\Sigma^+$ and $1\,^1\Pi$ states occurs near the distance of closest approach and then the flux is distributed to the excited $3\,^1\Sigma^+$ and $2\,^1\Pi$ states during the outgoing part of the collision. The cross section reaches a value of $\sim 1.3\times10^{-16}\,\mathrm{cm}^2$ at 6 keV/u, and it appears that it continues to grow as the collision energy increases. Experimental measurements for this system would be useful.

2. Electron capture by excited $Si^{2+}(^3P^o)$ ion impact

Calculated cross sections for electron capture by the lowest excited triplet $Si^{2+}(^3P^o)$ ion impact are presented in Fig. 3(b). There is no avoided crossing in this system between the initial and any electron-capture channels except for $R < 2.5a_0$, so the behavior of the total electron-capture cross section is similar to that of the ground $Si^{2+}(^1S)$ ion impact. However, in the case of the $Si^{2+}(^3P^o)$ ion, the cross section is somewhat larger than that of the $Si^{2+}(^1S)$ ion because the energy defect between the initial and final states is smaller than that for the ground singlet Si^{2+} ion. The cross sections of the $Si^{+}(3s^23p^1{:}\,^2P^o)$ state are dominant over that of the $Si^{+}(3s^13p^2{:}\,^4P)$ state at all collision energies considered. Again, we find mild oscillations both in the total and partial cross sections of the $Si^{+}(3s^23p^1{:}\,^2P^o)$ and $Si^{+}(3s^13p^2{:}\,^4P)$ states, but the behavior is somewhat complex compared to the case of the ground singlet $Si^{2+}(^1S)$ ion. This feature is a manifestation of a weaker coupling between the two electron-capture channels because of the larger asymptotic energy splittings as compared to the singlet case.

As seen in Fig. 1(b) the potential energy of the $1\,^3\Sigma^+$ state begins to approach that of the $1\,^3\Sigma^-$ state at small internuclear distances below $3a_0$. However, the transition between these two Σ states is forbidden by the symmetry conservation except for the indirect two-step process through Π states, which function as intermediaries. Hence, to a reasonable approximation, the electron capture process is still considered to be similar to the case of the ground singlet $Si^{2+}(^1S)$ ion impact. The cross section reaches a value of $2\times10^{-16}\,\mathrm{cm}^2$ at 6 keV/u, and it begins to level off at higher energies.

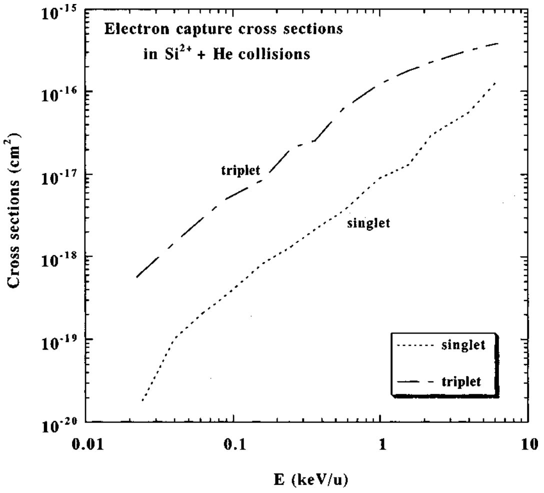

FIG. 4. Total electron-capture cross sections for the singlet (initial ground-state) and triplet (initial metastable-state) manifolds.

Both total cross sections for the singlet and triplet manifold are included in Fig. 4. The magnitude for the triplet cross sections are consistently larger than those of the singlet in the entire energy range studied. However, the singlet cross sections approach those of the triplet as the collision energy increases above a few keV/u, and they may reverse their order at much higher energies.

IV. RATE COEFFICIENTS

The present calculations are not intended to evaluate the rate coefficient accurately, but they are found to vary from $10^{-12}\,\mathrm{cm}^3/\mathrm{sec}$ at 6×10^5 K to $10^{-8}\,\mathrm{cm}^3/\mathrm{sec}$ at 2×10^8 K for both the singlet and triplet processes.

Although the charge of the Si^{q+} ions and the calculated collision energies are different, it is relevant and important to compare our results with those of the [Si^{3+}, Si^{4+}+He] systems studied so far. The results of the [Si^{4+}+He] system by Butler and Dalgarno [6] are almost independent of the temperature, but both the rate constants obtained by Opradolce, McCarroll, and Valiron [7], and Stancil *et al.* [8] increase with temperature. All these results have similar values ($\sim 10^{-9}\,\mathrm{cm}^3/\mathrm{s}$) at a temperature of $T = 10^4$ K. Opradolce, McCarroll, and Valiron and Stancil *et al.* calculated the rate constant at temperatures lower than 5×10^4 K, but the collision energies for which we calculated correspond to higher temperatures approximately in the region of $10^6 - 10^8$ K. However, the temperature dependence of our rate constants shows a more rapid increase than that of Opradolce, McCarroll, and Valiron and Stancil *et al.* Extrapolation of our results seems to suggest that the rate constant of the [Si^{2+}+He] system is smaller by about two to three orders of magnitude than that of the [Si^{4+}+He] at the temperature 5×10^4 K. This prediction is not surprising because there is no strong avoided crossing between the initial and electron-capture channels in the present [Si^{2+}+He] system, while there is an avoided crossing at the appropriate internuclear distance in the case of the [Si^{4+}+He] system, making electron capture more effective.

V. CONCLUSION

We have investigated electron capture in collisions of Si^{2+} ions with He atoms in the collision energy range from 0.02–6 keV/u based on a molecular representation. We have considered electron capture both by the ground singlet and metastable triplet Si^{2+} ions. The capture cross section by the ground singlet Si^{2+} ion continues to increase with increasing collision energy, and reaches a value of $1.3\times10^{-16}\,\mathrm{cm}^2$, while that by the metastable triplet ion is found to be large with a magnitude of $4\times10^{-16}\,\mathrm{cm}^2$ at the highest energy studied. Weak, but conspicuous, oscillatory structures are found for both cases, which are due to multichannel interferences. The present rate coefficient for the ground singlet Si^{2+} ion impact is probably much smaller than $\sim10^{-12}\,\mathrm{cm}^3/\mathrm{s}$ at the temperature 10^4 K because of its endothermicity of 96 000 K. This value is far smaller than those calculated for the [Si^{4+}+He] system.

ACKNOWLEDGMENTS

This work was supported in part by a Grant-in-Aid for Scientific Research (c) (07640527) and by that on Priority Area ''Atomic Physics of Multicharged Ions'' (Area No. 239/05238204) from the Ministry of Education of Japan (01540312). Financial support by the Deutsche Forschungsgemeinschaft (Grant No. Bu 450/7) and the Fonds der Chemischen Industrie is gratefully acknowledged. P.C.S. acknowledges support from U.S. DoE contract DE-ACO5-96OR22464 to Lockheed Martin Energy Research Corporation. M.K., J.P.G., and R.J.B. appreciate financial support by the US NSF through the Institute for Theoretical Atomic and Molecular Physics, Harvard-Smithsonian Center for Astrophyscs. Finally, M.K. acknowledges support from the Deutsche Akademische Austauschdienst (DAAD) through Universität Wuppertal during the time when much of this study was performed.

---

[1] W. Fritsch and H. Tawara, Nucl. Fusion **30**, 373 (1990).
[2] B. Herrero, I. L. Cooper, and A. S. Dickinson, J. Phys. B **29**, 5583 (1996).
[3] W. Wu and C. C. Havener, J. Phys. B **30**, L213 (1997).
[4] N. J. Clarke, P. C. Stancil, B. Zygelman, and D. L. Cooper, J. Phys. B **31**, 533 (1998).
[5] M. Pieksma, M. Gargaud, R. McCarroll, and C. C. Havener, Phys. Rev. A **54**, R13 (1996).
[6] S. E. Butler and A. Dalgarno, Astrophys. J. **241**, 838 (1980).
[7] L. Opradolce, R. McCarroll, and P. Valiron, Astron. Astrophys. **148**, 229 (1985).
[8] P. C. Stancil, B. Zygelman, N. J. Clarke, and D. L. Cooper, Phys. Rev. A **55**, 1064 (1997).
[9] P. Honvault, M. C. Bacchus-Montabonel, M. Gargaud, and R. McCarroll, Chem. Phys. **238**, 401 (1998).
[10] P. C. Stancil, N. J. Clarke, B. Zygelman, and D. L. Cooper, J. Phys. B **32**, 1523 (1999).
[11] M. C. Bacchus-Montabonel and P. Ceyzeriat, Phys. Rev. A **58**, 1162 (1998).
[12] Z. Fang and V. H. S. Kwong, Phys. Rev. A **59**, 342 (1999).
[13] Z. Fang and V. H. S. Kwong, Astrophys. J. **483**, 527 (1997).
[14] M. Kimura and N. F. Lane, in *Advances in Atomic, Molecular, and Optical Physics*, edited by D. R. Bates and B. Bederson (Academic, New York, 1989), Vol. 26, p. 79.
[15] N. Shimakura and M. Kimura, Phys. Rev. A **48**, 3652 (1991).
[16] M. Kimura, J. P. Gu, G. Hirsch, and R. J. Buenker, Phys. Rev. A **51**, 2063 (1995).
[17] M. Kimura, J. P. Gu, G. Hirsch, and R. J. Buenker, Phys. Rev. A **55**, 2778 (1997).
[18] M. Larsson, J. Chem. Phys. **86**, 5018 (1987).
[19] K. K. Sunil, J. Lin, H. Siddiqui, P. E. Siska, K. D. Jordan, and R. Shepard, J. Chem. Phys. **78**, 6190 (1983).
[20] A. Metropoulos, Y. Li, G. Hirsch, and R. J. Buenker, Chem. Phys. Lett. **198**, 266 (1992).
[21] R. J. Buenker and S. D. Peyerimhoff, Theor. Chim. Acta **35**, 33 (1974); **39**, 217 (1975); R. J. Buenker, Int. J. Quantum Chem. **29**, 435 (1986).
[22] R. J. Buenker, in *Proceedings of the Workshop on Quantum Chemistry and Molecular Physics, Wollongong, Australia*, edited by P. G. Burton (University Press, Wollongong, Australia, 1980); in *Studies in Physical and Theoretical Chemistry*, edited by R. Carbo (Elsevier, Amsterdam, 1981), Vol. 21, p.17; R. J. Buenker and R. A. Phillips, J. Mol. Struct.: THEOCHEM **123**, 291 (1985).
[23] G. Hirsch, P. J. Bruna, R. J. Buenker, and S. D. Peyerimhoff, Chem. Phys. **45**, 335 (1980).
[24] S. Bashkin and J. R. Stoner, Jr., *Atomic Energy Levels and Grotrian Diagrams I* (North-Holland, Amsterdam, 1975).
[25] M. W. Wong and L. Radom, J. Am. Chem. Soc. **110**, 2375 (1988).
[26] E. D. Jemmis, M. W. Wong, H. B. Buergi, and L. Radom, J. Mol. Struct.: THEOCHEM **261**, 385 (1992).
[27] P. Pyykko, Mol. Phys. **67**, 871 (1989).
[28] D. R. Schultz, C. O. Reinhold, and P. S. Krstic, Phys. Rev. Lett. **78**, 2720 (1997).